Supporting Information

for

O_2 activation by non-heme thiolate-based dinuclear Fe complexes

Lianke Wang,[a,b] Marcello Gennari,[b,*] Fabián G. Cantú Reinhard,[c] Sandeep K. Padamati,[b,d] Christian Philouze,[b] David Flot,[e] Serhiy Demeshko,[f] Wesley Browne,[d] Franc Meyer,[f] Sam P. de Visser,[c,*] Carole Duboc[b,*]

[a] *Institutes of Physical Science and Information Technology, Anhui University, 230601, Hefei, Anhui, P. R. China*
[b] *Univ. Grenoble Alpes, CNRS UMR 5250, DCM, F-38000 Grenoble, France*
[c] *Manchester Institute of Biotechnology and Department of Chemical Engineering and Analytical Science, The University of Manchester, 131 Princess Street, Manchester M1 7DN, United Kingdom*
[d] *Molecular Inorganic Chemistry, Stratingh Institute for Chemistry, Faculty of Science and Engineering, University of Groningen, Nijenborgh 4, 9747AG, Groningen, The Netherlands*
[e] *ESRF European Synchrotron 71, Ave Martyrs Grenoble, Grenoble, France*
[f] *University of Göttingen, Institute of Inorganic Chemistry, Tammannstrasse 4, D- 37077 Göttingen, Germany*

* corresponding authors: carole.duboc@univ-grenoble-alpes.fr; marcello.gennari@univ-grenoble-alpes.fr, sam.devisser@manchester.ac.uk

Crystallographic tables

Table S1. Crystallographic Data for **[Fe_2^S]**·0.5CH_3CN·0.75Et_2O and **[Fe_2^O]**.

	[Fe_2^S]·0.5CH_3CN·0.75Et_2O	**[Fe_2^O]**
empirical formula	2[$C_{80}H_{69}Fe_2N_{4.5}O_{0.75}S_4$]	$C_{76}H_{60}Fe_2N_4OS_4$
formula weight	2690.67	1285.30
crystal system	monoclinic	monoclinic
space group	P 21/n	P 21/c
a Å	26.347(5)	19.625(4)
b Å	19.908(4)	21.001(4)
c Å	26.789(5)	17.413(4)
α °	90	90
β °	106.47(3)	91.93(3)
γ °	90	90
V $Å^3$	13475(5)	7173(2)
Z	4	4
T K	200	100
D_{calcd} $g \cdot cm^{-3}$	1.326	1.1902
μ mm^{-1}	0.605	0.601
θ range °	1.401-25.000	1.065-32.352
total no. data	129233	109409
no.unique data	23118	17888
no. params refined	1709	939
R_1	0.0745	0.1447
wR_2	0.1608	0.3618
GOF	1.056	1.1019

Table S2. Selected bond lengths (Å) and angles (°) for the two crystallographically independent units of **[Fe_2^S]**·0.5CH_3CN·0.75Et_2O.

Fe1A-S1A	2.3382(15)	Fe2A-S2A	2.3959(15)
Fe1A-S2A	2.3905(16)	Fe2A-S3A	2.3985(17)
Fe1A-S3A	2.4243(17)	Fe2A-S4A	2.3632(17)
Fe1A-N1A	2.145(4)	Fe2A-N3A	2.235(4)
Fe1A-N2A	2.240(5)	Fe2A-N4A	2.129(4)
S2A-Fe1A-S3A	91.70(5)	S2A-Fe2A-S3A	92.21(5)
S1A-Fe1A-S2A	87.50(5)	S4A-Fe2A-S2A	104.70(6)
S1A-Fe1A-S3A	102.75(6)	S4A-Fe2A-S3A	90.05(5)
N2A-Fe1A-S2A	92.60(12)	N3A Fe2A-S2A	116.22(12)
N2A-Fe1A-S1A	136.12(12)	N3A-Fe2A-S4A	138.88(12)
N2A-Fe1A-S3A	121.09(12)	N3A-Fe2A-S3A	92.16(11)
N1A-Fe1A-S2A	162.69(14)	N4A-Fe2A-S2A	101.62(12)
N1A-Fe1A-S1A	91.75(12)	N4A-Fe2A-S4A	91.89(13)
N1A-Fe1A S3A	105.31(13)	N4A-Fe2A-S3A	165.05(12)
N1A-Fe1A-N2A	76.04(17)	N4A-Fe2A-N3A	76.71(16)
Fe1A-Fe2A	3.2544(12)		
Fe1B-S1B	2.3295(15)	Fe2B-S2B	2.3992(16)
Fe1B-S2B	2.4047(17)	Fe2B-S3B	2.4110(18)
Fe1B-S3B	2.4092(16)	Fe2B-S4B	2.334(2)
Fe1B-N1B	2.132(4)	Fe2B-N3B	2.215(5)
Fe1B-N2B	2.242(5)	Fe2B-N4B	2.123(5)
S1B-Fe1B-S2B	88.98(5)	S2B-Fe2B-S3B	95.32(5)
S1B-Fe1B-S3B	105.42(6)	S4B-Fe2B-S2B	110.43(7)
S2B-Fe1B-S3B	95.22(6)	S4B-Fe2B-S3B	86.76(6)
N2B-Fe1B-S1B	132.55(12)	N3B-Fe2B-S2B	116.37(13)
N2B-Fe1B-S2B	91.73(12)	N3B-Fe2B-S3B	92.82(14)
N2B-Fe1B-S3B	121.71(12)	N3B-Fe2B-S4B	133.01(14)
N1B-Fe1B-S1B	88.95(12)	N4B-Fe2B-S2B	105.96(14)
N1B-Fe1B-S2B	160.17(13)	N4B-Fe2B-S3B	158.61(14)
N1B-Fe1B-S3B	104.34(13)	N4B-Fe2B-S4B	87.73(14)
N1B-Fe1B-N2B	75.34(17)	N4B-Fe2B-N3B	76.06(19)
Fe1B-Fe2B	3.2179(13)		

Table S3. Selected bond lengths (Å) and angles (°) for **[Fe_2^O]**.

Fe1-S2	2.348(3)	Fe2-S4	2.341(3)
Fe1-S1	2.288(3)	Fe2-S3	2.317(3)
Fe1-O1	1.807(6)	Fe2-O1	1.777(7)
Fe1-N1	2.224(7)	Fe2-N3	2.132(7)
Fe1-N2	2.157(7)	Fe2-N4	2.168(8)
S1-Fe1-S2	86.30(11)	S3-Fe2-S4	80.30(12)
O1-Fe1-S2	114.2(2)	O1-Fe2-S4	113.4(2)
O1-Fe1-S1	102.3(2)	O1-Fe2-S3	115.1(3)
O1-Fe1-N1	110.5(3)	O1-Fe2-N3	98.7(3)
O1-Fe1-N2	97.1(3)	O1-Fe2-N4	105.3(3)
N1-Fe1-S2	134.4(2)	N3-Fe2-S4	147.7(2)
N1-Fe1-S1	92.9(2)	N3-Fe2-S3	89.2(2)
N2-Fe1-S2	89.6(2)	N3-Fe2-N4	76.7(3)
N2-Fe1-S1	160.16(19)	N4-Fe2-S4	91.3(2)
N2-Fe1-N1	76.2(3)	N4-Fe2-S3	138.8(2)

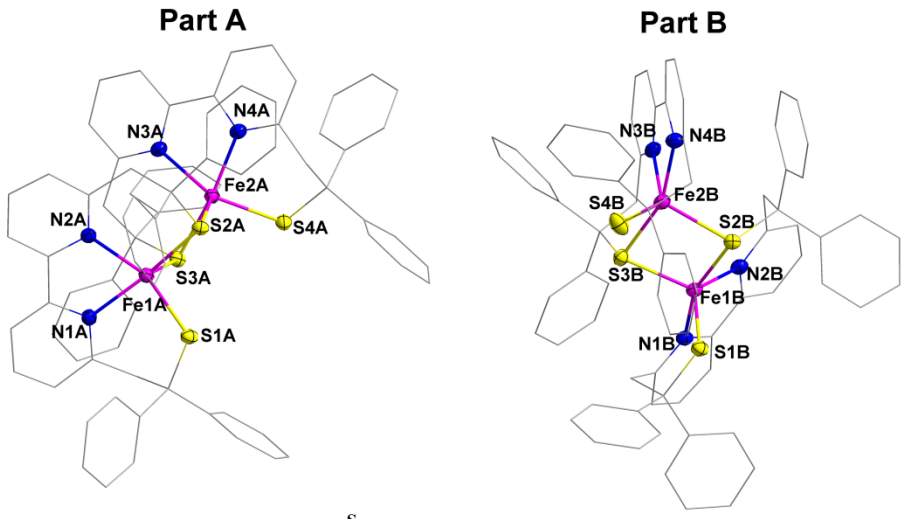

Figure S1. X-ray crystal structure of **[Fe_2^S]**·0.5CH_3CN·0.75Et_2O displaying both crystallographically independent units. The thermal ellipsoids of the metal cores are drawn at 30% probability level. All hydrogen atoms and solvent molecules are omitted for clarity.

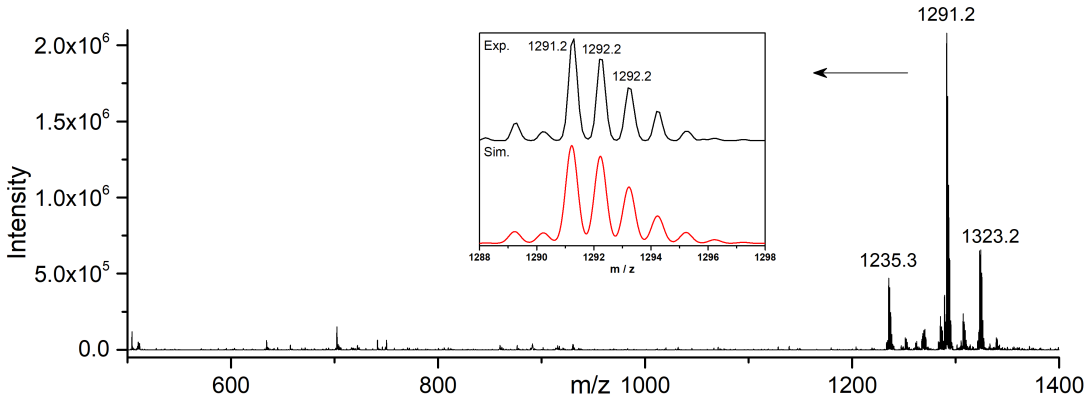

Figure S2. Full ESI-mass spectrum of **[Fe_2^S]** in CH_3CN (the inset displays a zoom of the molecular peak, m/z 1291.2, **[Fe_2^S]**+Na^+, experimental and simulated data).

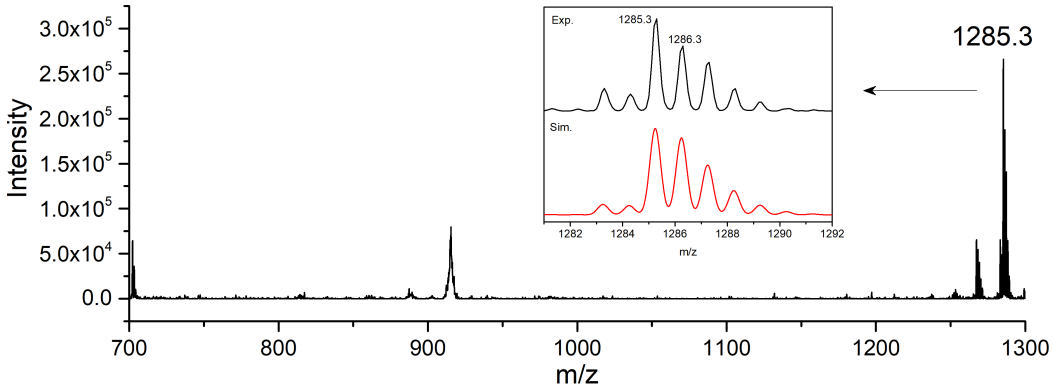

Figure S3. Full ESI-mass spectrum of $[\mathbf{Fe_2^{OH}}]^+$ generated from $[\mathbf{Fe_2^{SH}}]^+$ and O_2 in CH_3CN (the inset displays a zoom of the molecular peak, m/z 1285.3, $[\mathbf{Fe_2^{OH}}]^+$, experimental and simulated data).

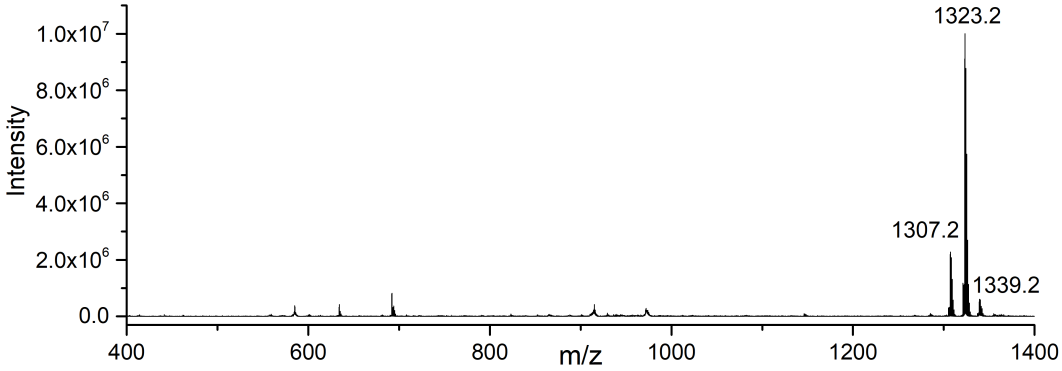

Figure S4. Full ESI-mass spectrum of $[\mathbf{Fe_2^{O}}]$ generated from $[\mathbf{Fe_2^{S}}]$ and $^{16}O_2$ in acetonitrile.

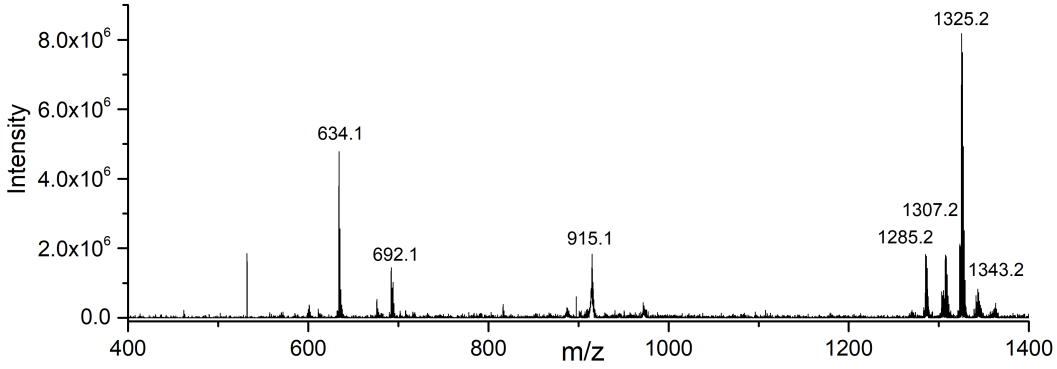

Figure S5. Full ESI-mass spectrum of $[\mathbf{Fe_2^{O}}]^{18}$ generated from $[\mathbf{Fe_2^{S}}]$ and $^{18}O_2$ in acetontrile.

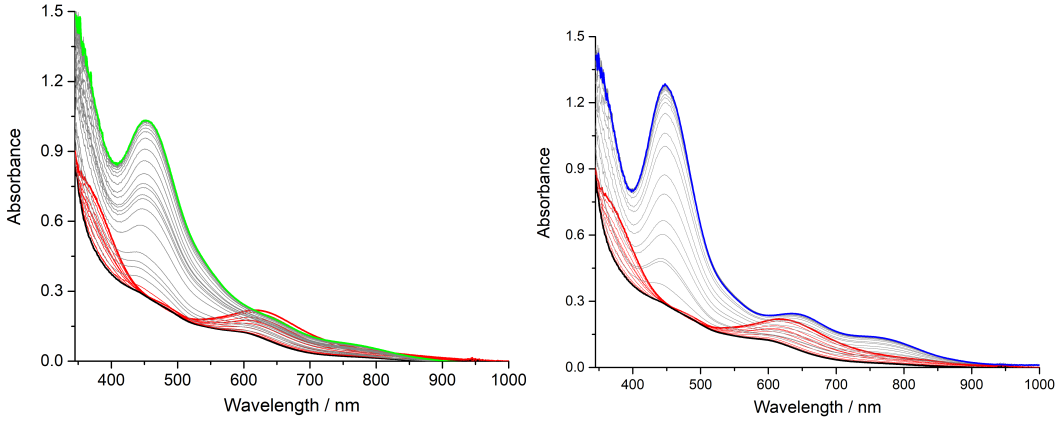

Figure S6. UV-vis spectra of **[Fe_2^S]** (1 cm path length, scan every 1 s) in MeCN before (red) and after (black) addition of 1 (left) and 2 (right) equivalent of $LutH^+$, followed by exposing to O_2.

DFT calculations

Figure S7. Optimized structures for Schemes 3-5 (except for the structures of $[Fe_2^{SH}]^+$, $[Fe_2^{OO./SH}]^+$ and $[Fe_2^{OO/SH}]^+$, which were previously reported{Wang, 2019 #1}) calculated at the UBLYP/BS1 level of theory in Gaussian with phenyl substituents. Antiferromagnetic configurations only with bond lengths in angstroms. For ferromagnetic structures, see Tables and Cartesian coordinates.

a) $[Fe_2^{S}]$

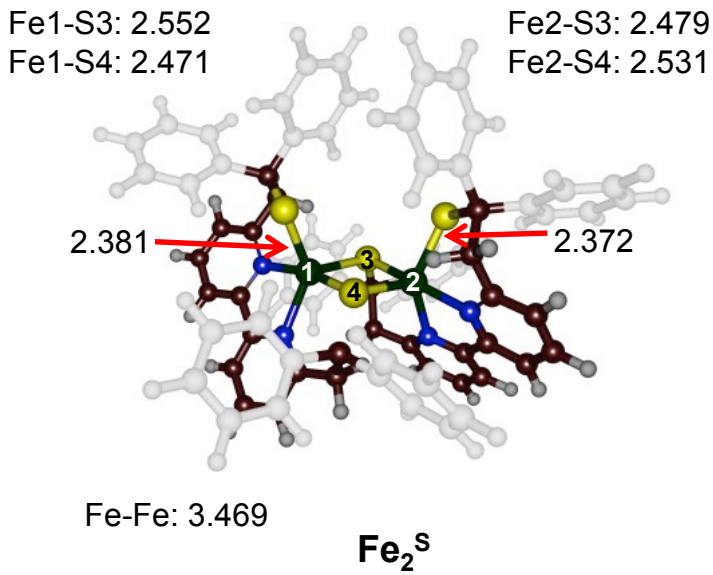

b) $[Fe_2^{OO\cdot}]$

Fe1-S3: 2.680
Fe1-S4: 2.514

Fe2-S3: 2.343
Fe2-S4: 2.631

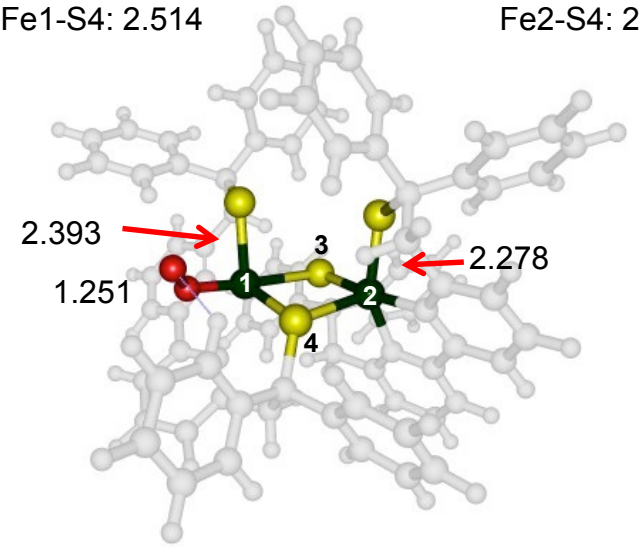

Fe-O: 1.881
Fe-Fe: 3.661 **$[Fe_2^{OO\circ}]$**

c) $[Fe_2^{OO}]$

Fe1-O4: 1.885

Fe2-O3: 1.890
O3-O4: 1.424

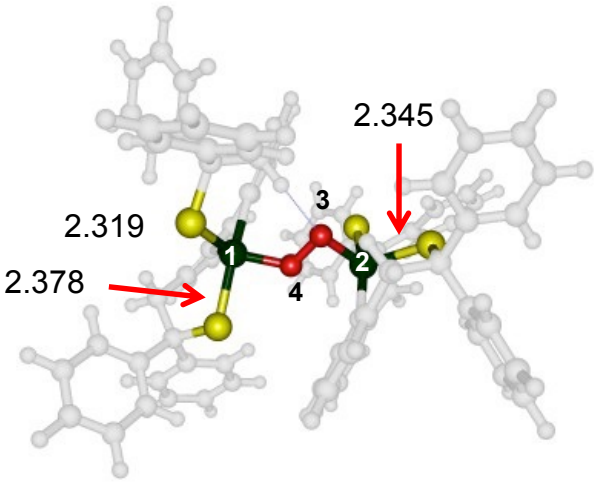

Fe-Fe: 4.214

$[Fe_2^{OO}]$

d) **[$Fe_2^{(O)2}$]**

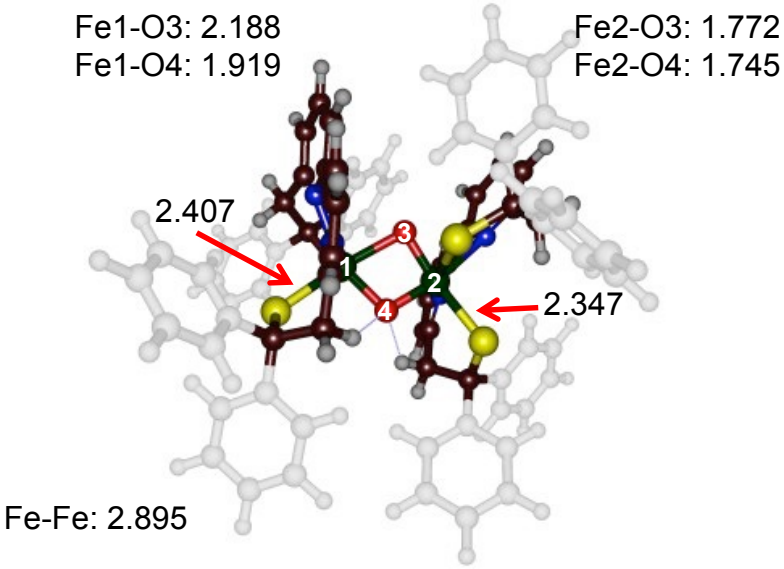

[Fe_2 $^{(O)2}$]

e) **[Fe_2^{O}]**

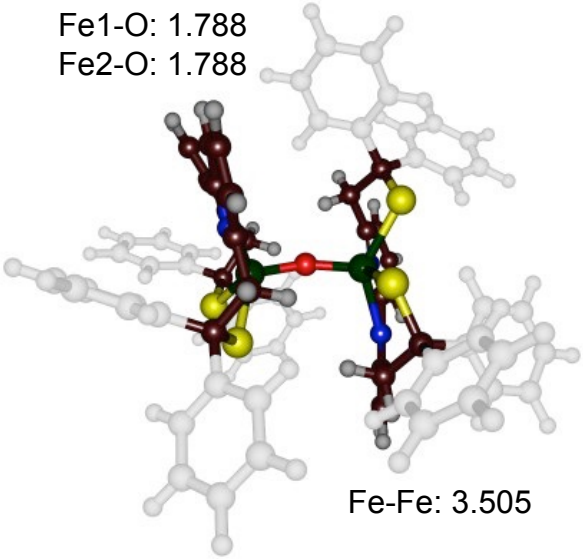

[Fe_2^{O}]

Table S4. Absolute energies (in au) of antiferromagnetic (AF) states of complexes in Schemes 3-5. Data obtained with the **small model** with methyl substituents at the **UBLYP** level of theory in Gaussian-09.

		E [BS1]	ZPE [BS1]	G [BS1]	Esolv [BS2]	Esolv [BS2] + ZPE
[Fe_2^{S}]	AF	-3456.2330	-3455.5167	-3455.5944	-3456.9033	-3456.1870
[$Fe_2^{OO\cdot}$]	AF	-3606.5535	-3605.8314	-3605.9105	-3607.2813	-3606.5591
[Fe_2^{OO}]	AF	-3606.5721	-3605.8498	-3605.9313	-3607.3072	-3606.5849
[$Fe_2^{(O)2}$]	AF	-3606.6107	-3605.8882	-3605.9664	-3607.3493	-3606.6267
[Fe_2^{O}]	AF	-3531.4466	-3530.7281	-3530.8107	-3532.1682	-3531.4498

Table S5. Relative energies along the reaction mechanism in Schemes 3-5. All values are in kcal mol^{-1}. Data obtained with the **small model** with methyl substituents at the **UBLYP** level of theory in Gaussian-09.

		ΔE	ΔE+ZPE	ΔG	ΔE	ΔE+ZPE	ΔE_{solv}	ΔE_{solv}+ZPE
		[BS1]	[BS1]	[BS1]	[BS2]	[BS2]	[BS2]	[BS2]
[Fe_2^{S}]	AF	0.0	0.0	0.0	0.0	0.0	0.0	0.0
[$Fe_2^{OO\cdot}$]	AF	-5.7	-4.1	7.6	-2.9	-1.4	-5.4	-3.8
[Fe_2^{OO}]	AF	-17.3	-15.7	-5.5	-18.2	-16.6	-21.7	-20.0
[$Fe_2^{(O)2}$]	AF	-41.5	-39.8	-27.5	-44.8	-43.1	-48.1	-46.3
2* **[Fe_2^{OO}]**$_{AF}$ → O_2+ 2* **[Fe_2^{O}]**$_{AF}$		-38.0	-40.6	-54.5	-45.8	-48.4	-57.4	-60.0

Table S6. Group spin densities of the complexes from Schemes 3-5 as calculated at various levels of theory. Data obtained with the **small model** with methyl substituents at the **UBLYP** level of theory in Gaussian-09.

		BLYP/BS1			BLYP/BS2			BLYP+PCM/BS2		
		ρ Fe1	ρ Fe2	All Else	ρ Fe1	ρ Fe2	All Else	ρ Fe1	ρ Fe2	All Else
[Fe_2^{S}]	AF	2.00	-2.00	0.00	1.96	-1.96	0.00	1.91	-1.91	0.00
[$Fe_2^{OO\cdot}$]	AF	0.82	-2.01	1.18	0.78	-1.92	1.15	0.84	-1.88	1.04
[Fe_2^{OO}]	AF	0.89	-0.89	0.00	0.81	-0.80	0.00	0.78	-0.78	0.00
[$Fe_2^{(O)2}$]	AF	1.47	-1.43	-0.04	1.34	-1.30	-0.04	1.37	-1.33	-0.03
[Fe_2^{O}]	AF	2.20	-2.20	0.00	2.23	-2.24	0.01	2.25	-2.26	0.01

Table S7. Absolute energies (in au) and spin densities (at BS1) of various ferromagnetic and antiferromagnetic states of complex **[Fe_2^{S}]**,. Data obtained with the **small model** with methyl substituents at **UB3LYP** in Gaussian-09. A star on ID refers to the selected complex as best.

ID	E [BS1]	ZPE [BS1]	G [BS1]	Esolv [BS2]	Spin Fe1	Spin Fe2	Spin Ligand
[Fe_2^{S}]$_{,AF}$*	-3457.195305	-3456.457952	-3456.537581	-3457.826967	3.6	-3.6	0.0
[Fe_2^{S}]$_{,F5}$	-3457.173744	-3456.435104	-3456.514098	-3457.813186	3.6	0.0	0.3
[Fe_2^{S}]$_{,F7}$	-3457.187307	-3456.449003	-3456.528696	-3457.813186	3.6	2.1	0.3
[Fe_2^{S}]$_{,F9}$	-3457.194143	-3456.456870	-3456.538844	-3457.825798	3.6	3.6	0.8
[Fe_2^{S}]$_{F11}$	-3457.147392	-3456.411386	-3456.492725	-3457.783347	3.8	3.6	2.6

Table S8. Absolute energies (in au) and spin densities (at BS1) of various ferromagnetic and antiferromagnetic states of complex **[$Fe_2^{OO\cdot}$]**. Data obtained with the **small model** with methyl substituents at **UB3LYP** in Gaussian-09. A star on ID refers to the selected complex as best.

ID	E [BS1]	ZPE [BS1]	G [BS1]	Esolv [BS2]	Spin Fe1	Spin Fe2	Spin Ligand
[$Fe_2^{OO\cdot}$]$_{,AF}$*	-3607.490739	-3606.746237	-3606.826100	-3608.171501	2.8	-2.1	-0.7
[$Fe_2^{OO\cdot}$]$_{,F5}$	-3607.486315	-3606.742674	-3606.828502	-3608.157499	2.1	0.0	1.9
[$Fe_2^{OO\cdot}$]$_{,F7}$	-3607.500273	-3606.756814	-3606.843672	-3608.170884	2.1	2.1	1.7
[$Fe_2^{OO\cdot}$]$_{,F9}$	-3607.507508	-3606.764891	-3606.853321	-3608.183216	3.6	2.1	2.3
[$Fe_2^{OO\cdot}$]$_{,F11}$	-3607.514655	-3606.773189	-3606.861298	-3608.195802	3.6	3.6	2.8

*Note: Complexes F5-F11 result in dissociation of molecular O_2 off the complex.

Table S9. Absolute energies (in au) and spin densities (at BS1) of various ferromagnetic and antiferromagnetic states of complex **[Fe_2^{OO}]**. Data obtained with the **small model** with methyl substituents at **UB3LYP** in Gaussian-09. A star on ID refers to the selected complex as best.

ID	E [BS1]	ZPE [BS1]	G [BS1]	Esolv [BS2]	Spin Fe1	Spin Fe2	Spin Ligand
[Fe_2^{OO}]$_{,AF}$*	-3607.521135	-3606.777269	-3606.859218	-3608.209409	2.9	-2.9	-0.1
[Fe_2^{OO}]$_{,F5}$	-3607.503816	-3606.758935	-3606.842328	-3608.192450	2.9	1.2	-0.1
[Fe_2^{OO}]$_{,F7}$	-3607.499966	-3606.755450	-3606.840082	-3608.197228	3.7	1.1	1.2
[Fe_2^{OO}]$_{,F9}$	-3607.512214	-3606.768384	-3606.853547	-3608.212080	3.7	2.9	1.4
[Fe_2^{OO}]$_{,F11}$	-3607.507219	-3606.764020	-3606.850764	-3608.216507	3.7	3.7	2.5

Table S10. Absolute energies (in au) and spin densities (at BS1) of various ferromagnetic and antiferromagnetic states of complex **[$Fe_2(^{O)2}$]**. Data obtained with the **small model** with methyl substituents at **UB3LYP** in Gaussian-09. A star on ID refers to the selected complex as best.

ID	E [BS1]	ZPE [BS1]	G [BS1]	Esolv [BS2]	Spin Fe1	Spin Fe2	Spin Ligand
[$Fe_2(^{O)2}]_{,AF}$*	-3607.522758	-3606.779048	-3606.858632	-3608.224259	3.4	-3.4	0.0
[$Fe_2(^{O)2}]_{,F5}$	-3607.511199	-3606.766713	-3606.846362	-3608.200891	3.3	-1.1	1.7
[$Fe_2(^{O)2}]_{,F7}$	-3607.521386	-3606.776586	-3606.856738	-3608.217360	3.3	2.0	0.6
[$Fe_2(^{O)2}]_{,F9}$	-3607.513389	-3606.769438	-3606.850933	-3608.204249	3.8	2.0	2.2
[$Fe_2(^{O)2}]_{,F11}$	-3607.515173	-3606.772303	-3606.855018	-3608.211916	3.9	3.4	2.7

Table S11. Absolute energies (in au) and spin densities (at BS1) of various ferromagnetic and antiferromagnetic states of complex **[Fe_2^{O}]**. Data obtained with the **small model** with methyl substituents at **UB3LYP** in Gaussian-09. A star on ID refers to the selected complex as best.

ID	E [BS1]	ZPE [BS1]	G [BS1]	Esolv [BS2]	Spin Fe1	Spin Fe2	Spin Ligand
[$Fe_2^{O}]_{AF}$	-3532.391338	-3531.650001	-3531.731410	-3533.062831	2.9	-2.9	0.0
[$Fe_2^{O}]_{F5}$	-3532.375059	-3532.375059	-3531.714295	-3533.051284	3.8	-1.0	1.2
[$Fe_2^{O}]_{F7}$	-3532.372717	-3531.631170	-3531.713755	-3533.049788	3.8	1.1	1.1
[$Fe_2^{O}]_{F9}$	-3532.386013	-3531.645368	-3531.729926	-3533.065842	3.8	3.0	1.2
[$Fe_2^{O}]_{F11}$*	-3532.389758	-3531.649344	-3531.733952	-3533.075555	3.8	3.8	2.4

Table S12. Group spin densities of selected complexes from Schemes 3-5 as calculated at various levels of theory. Data obtained with the **small model** with methyl substituents at **UB3LYP** in Gaussian-09.

	BLYP/BS1			BLYP/BS2			BLYP+PCM/BS2		
#	ρ Fe1	ρ Fe2	All Else	ρ Fe1	ρ Fe2	All Else	ρ Fe1	ρ Fe2	All Else
[$Fe_2^{S}]_{,AF}$	3.63	-3.63	0.00	3.40	-3.40	0.00	3.41	-3.42	0.00
[$Fe_2^{OO\cdot}]_{,AF}$	2.82	-2.12	-0.70	2.43	-2.04	-0.39	2.44	-1.97	-0.48
[$Fe_2^{OO}]_{,AF}$	2.93	-2.86	-0.06	2.72	-2.68	-0.04	2.72	-2.69	-0.03
[$Fe_2(^{O)2}]_{,AF}$	3.41	-3.41	0.00	3.17	3.17	0.00	3.17	-3.17	0.00
[$Fe_2^{O}]_{F11}$	3.83	3.82	2.35	3.98	3.99	2.03	4.00	4.00	2.00

Table S13. Absolute energies (in au) of antiferromagnetic (AF) states of complexes in Schemes 3-5. Data obtained from the **large model** at **UB3LYP** in Gaussian-09.

#	Spin	E [BS1]	ZPE [BS1]	G [BS1]	Esolv [BS2]	Esolv [BS2]+ZPE
[Fe_2^{S}]	AF	-4991.006921	-4989.847868	-4989.963916	-4992.001491	-4990.842438
[$Fe_2^{OO\cdot}$]	AF	-5141.295988	-5140.130212	-5140.248071	-5142.331485	-5141.165710
[Fe_2^{OO}]	AF	-5141.319598	-5140.154675	-5140.276469	-5142.377973	-5141.213050
[$Fe_2^{(O)2}$]	AF	-5141.319465	-5140.155284	-5140.273918	-5142.381148	-5141.216967
[Fe_2^{O}]	AF	-5066.205488	-5065.042934	-5065.163351	-5067.239385	-5066.076831
Isolated MeCN	N/A	-132.751485	-132.7058	-132.72985	-132.7461	-132.7547

Table S14. Relative energies (in kcal/mol) of selected models of schemes 3-5. Data obtained with the **small model** with methyl substituents at **UB3LYP** in Gaussian-09.

ID	E [BS1]	ZPE [BS1]	G [BS1]	Esolv [BS2]	Esolv [BS2]+ZPE
$[Fe_2^{S}]_{,AF}$	0.0	0.0	0.0	0.0	0.0
$[Fe_2^{OO\cdot}]_{,AF}$	12.7	15.0	28.9	15.5	17.7
$[Fe_2^{OO}]_{,AF}$	-6.3	-4.5	8.1	-8.3	-6.4
$[Fe_2^{(O)2}]_{,AF}$	-7.3	-5.6	8.5	-17.6	-15.9
2* $[Fe_2^{OO}]_{,AF}$ $\rightarrow$ O_2+ 2* **$[Fe_2^{O}]_{F11}$**	-33.8	-35.8	-51.6	-64.5	-66.5

Note: Molecular O_2 energies were employed to complement relative energy vs complex **$[Fe_2^{S}]$**,

Table S15. Absolute energies (in kcal/mol) of selected models of scheme 1. Data obtained from the **large model** at **UB3LYP** in Gaussian-09.

ID	E [BS1]	ZPE [BS1]	G [BS1]	Esolv [BS2]	Esolv [BS2]+ZPC
$[Fe_2^{S}]_{,AF}$	-4991.006921	-4989.847868	-4989.963916	-4991.949959	-4990.790907
$[Fe_2^{OO\cdot}]_{,AF}$	-5141.295988	-5140.130212	-5140.248071	-5142.331485	-5141.165710
$[Fe_2^{OO}]_{,AF}$	-5141.319598	-5140.154675	-5140.276469	-5142.377973	-5141.213050
$[Fe_2^{(O)2}]_{,AF}$	-5141.319595	-5140.154686	-5140.276528	-5142.377929	-5141.213020
$[Fe_2^{O}]_{F11}$	-5066.205488	-5065.042934	-5065.163351	-5067.239385	-5066.076831

Table S16. Relative energies (in kcal/mol) of selected models of schemes 3-5. Data obtained from the **large model** at **UB3LYP** in Gaussian-09.

ID	E [BS1]	ZPE [BS1]	G [BS1]	Esolv [BS2]	Esolv [BS2]+ZPC
$[Fe_2^{S}]_{,AF}$	0	0	0	0	0
$[Fe_2^{OO\cdot}]_{,AF}$	17.3	19.1	30.5	25.4	27.3
$[Fe_2^{OO}]_{,AF}$	-4.5	-3.6	4.8	-15.6	-14.7
$[Fe_2^{(O)2}]_{,AF}$	2.5	3.4	14.3	-5.7	-4.9
2* **$[Fe_2^{OO}]_{,AF}$** $\rightarrow$ O_2+ 2***$[Fe_2^{O}]$**	-55.5	-56.1	-66.9	-58.6	-59.2

Figure S8. B3LYP/BS1 calculated IR spectra of selected structures.

IR spectrum of **[Fe_2^{OO}]** O^{16}:

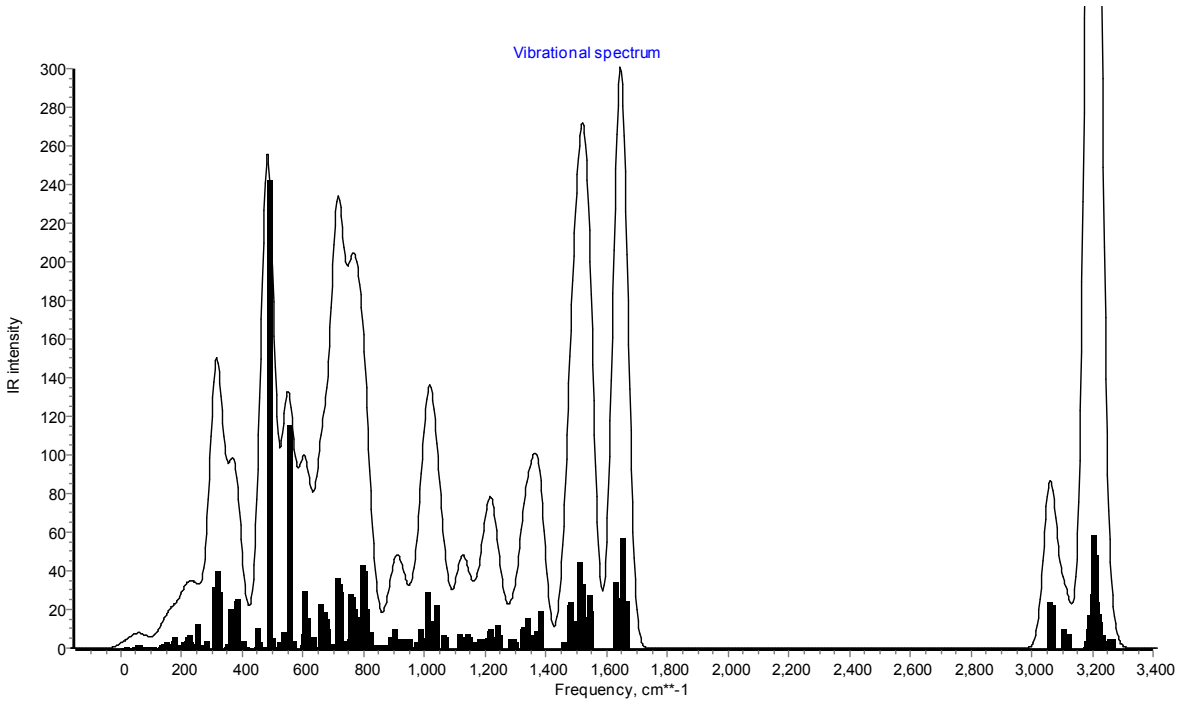

IR spectrum of **[Fe_2^{OO}]** O^{18}:

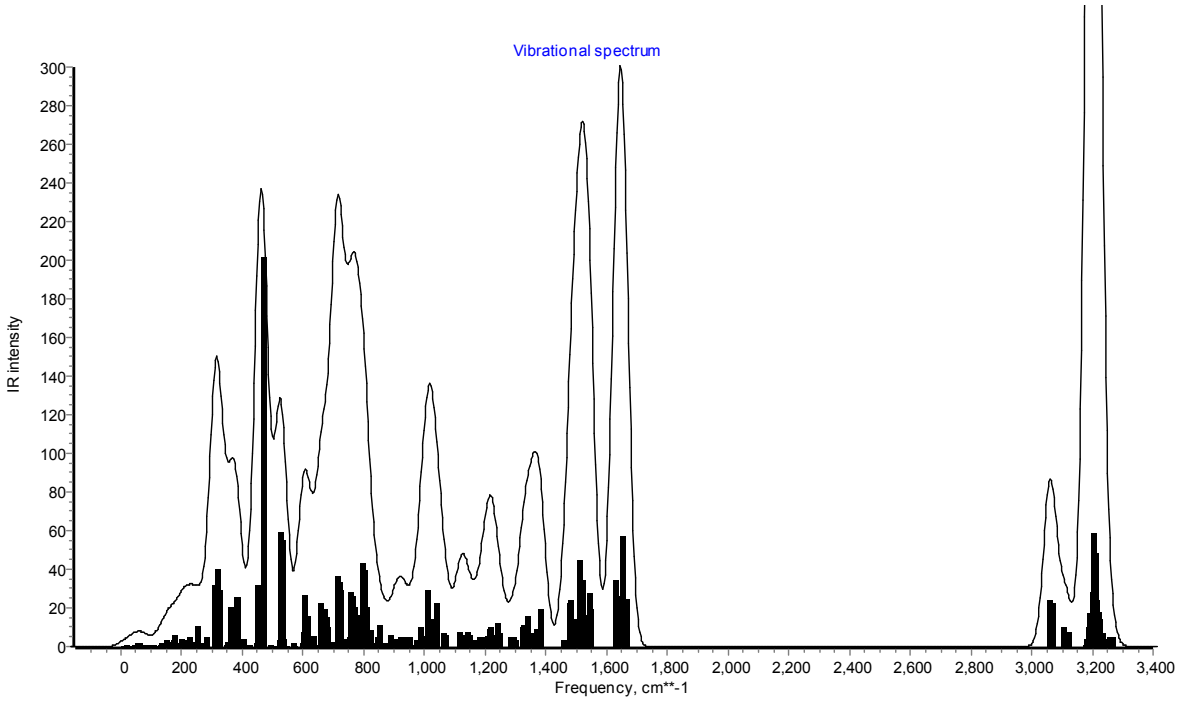

Raman spectrum of **[Fe_2^{OO}]** O^{16}:

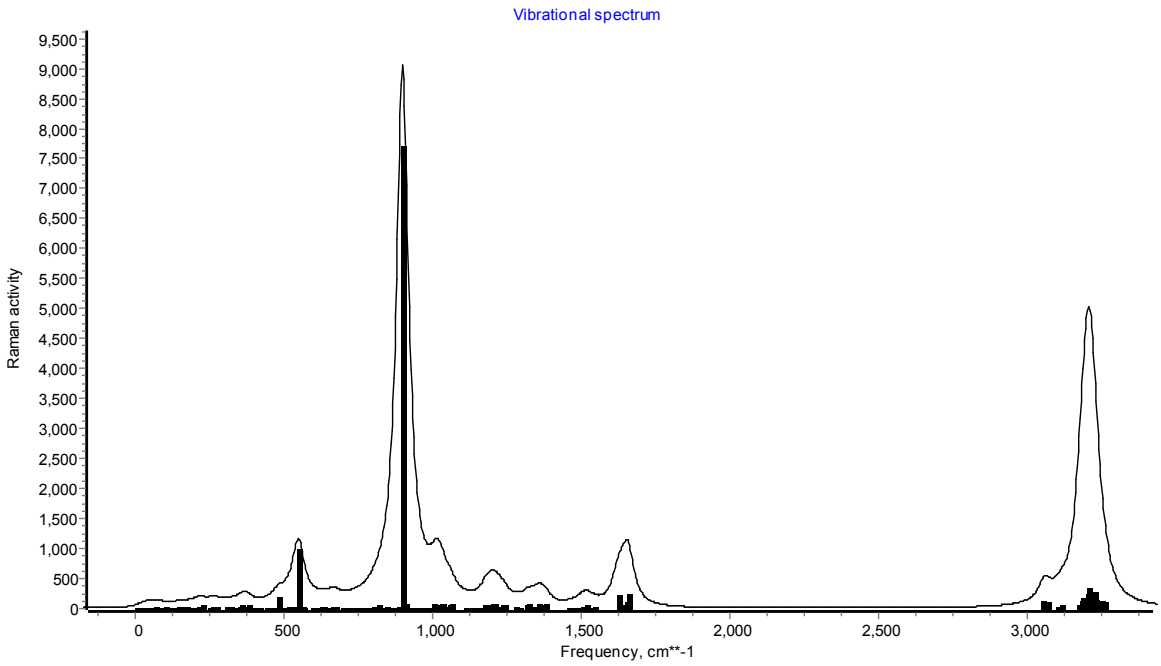

Table S17. Characterization of frequencies in IR and Raman spectra of **[Fe_2^{OO}]** with $^{16}O_2$ and $^{18}O_2$. Frequencies in wave numbers.

IR frequencies:	$^{16}O_2$	$^{16}O_2$		$^{18}O_2$	$^{18}O_2$
	IR freq	IR int		IR freq	IR int
S-Fe-O bend	307.39	12.5			
S-Fe-O bend	308.58	32.0			
S-Fe-O bend	311.15	12.1			
S-Fe-O bend	311.90	8.2			
Fe-O stretch	483.35	242.3		464.50	201.4
Fe-O stretch	551.08	115.2		524.50	59.4
O-O stretch	900.75	10.0		850.36	11.2

Figure S9. B3LYP/BS1 calculated IR spectra of selected structures.

IR spectrum of **[Fe_2^O]** O^{16}:

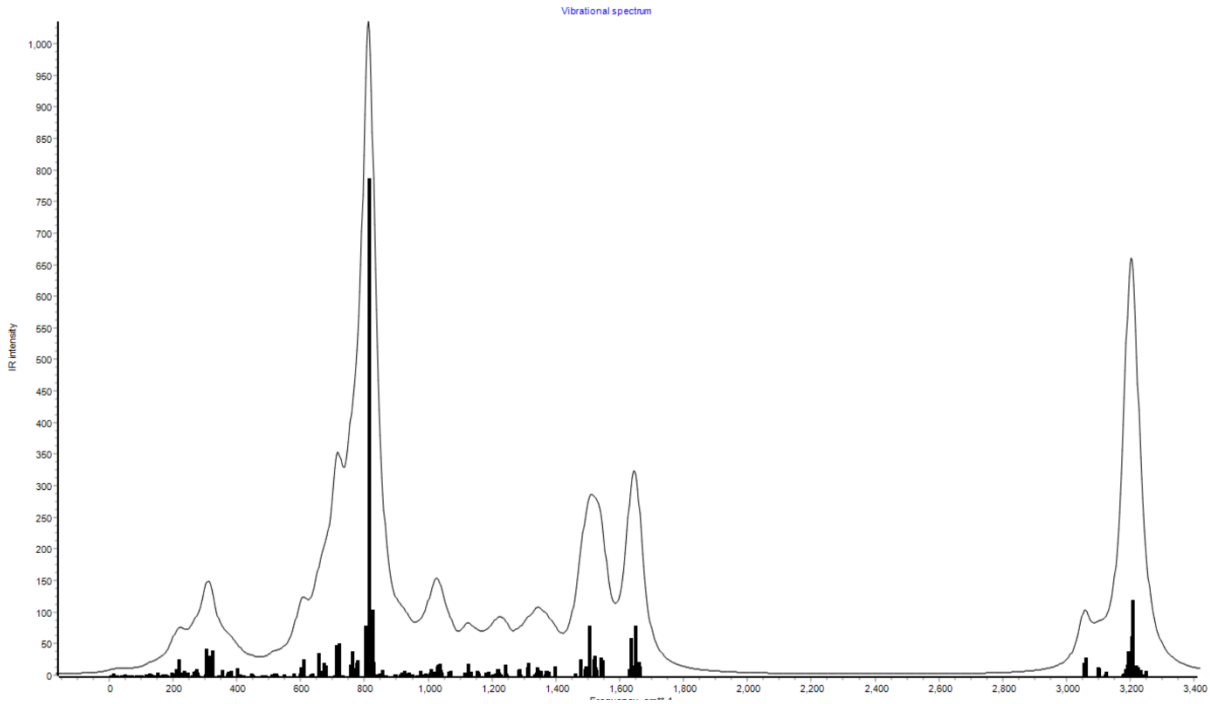

Raman spectrum of **[Fe_2^O]** O^{16}:

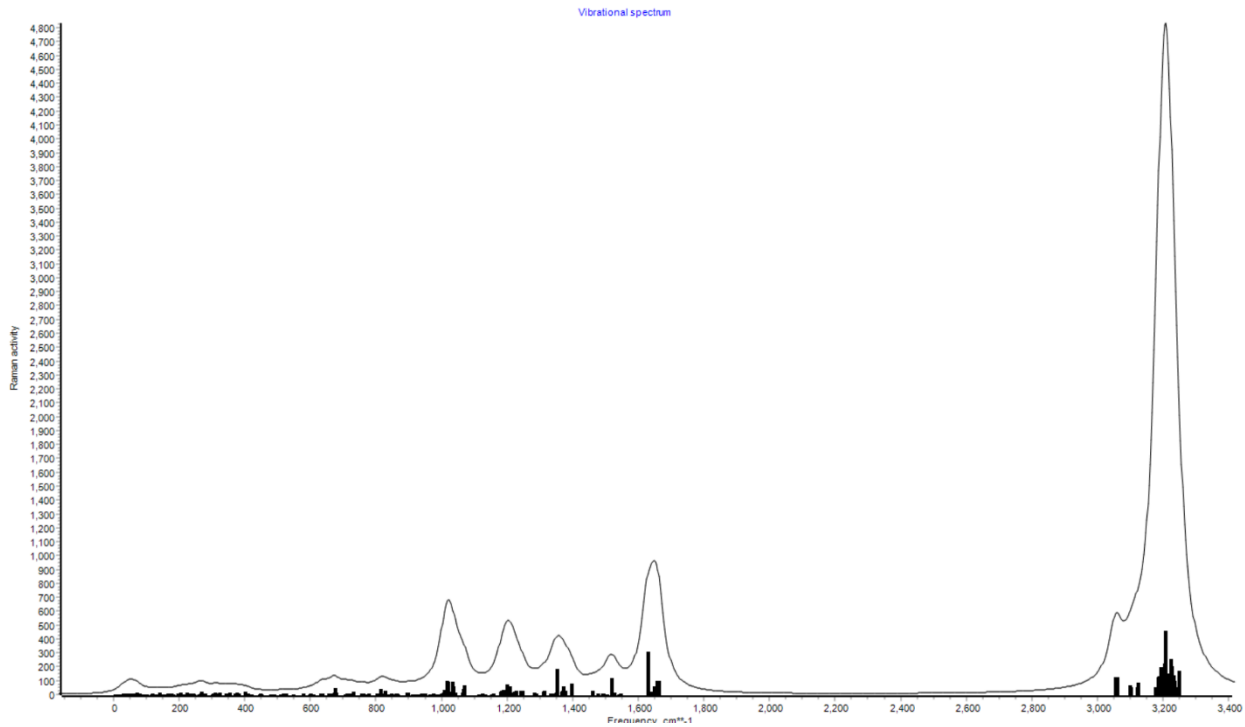

Table S18. Characterization of IR and Raman Intensities on **[Fe_2^O]**, frequencies in wave numbers.

IR frequencies	**[Fe_2^O]** O^{16}		
	IR freq	IR Intensity	Raman Intensity
Fe-O-Fe vibration	149.07	4.4208	1.6034
O Vibration	165.9333	1.1831	2.8324
Fe-O-Fe vibration	194.4084	4.7694	5.246
SFe-O-FeS Vibration	208.6508	9.5764	1.1659
SFe-O-FeS Vibration	218.1176	24.6289	1.4336
O Vibration	222.6664	3.6117	14.7891
SFe-O-FeS Vibration	302.2062	41.7378	4.2171
S – Ph Vibrations	309.8841	30.5718	2.8398
S – Ph Vibrations	321.0626	39.438	11.8412
Fe-O-Fe Vibration	398.904	11.3992	22.0675
Fe-O-Fe stretch	812.6341	786.7154	36.8733
Ph C-H Bond Bends	824.5046	103.3963	7.6047
Ph C-C Bond Streches	1504.38	78.4501	3.0453
Ph C-C Bond Streches	1647.233	78.7102	48.6016
Ph-CH Bond Strech	3206.097	118.5677	167.474